AGU PUBLICATIONS

Geochemistry, Geophysics, Geosystems

RESEARCH ARTICLE
10.1002/2015GC005955

**Key Points:**
- Cascadia margin methane plumes show elevated emissions at upper depth limit of gas hydrate stability
- Known plume depths on the U.S. Atlantic margin do not correlate to gas hydrate stability depths
- Methane hydrate decomposition on North American margins still remains an open question

**Supporting Information:**
- Supporting Information S1

**Correspondence to:**
H. P. Johnson,
paulj@uw.edu

**Citation:**
Johnson, H. P., U. K. Miller, M. S. Salmi, and E. A. Solomon (2015), Analysis of bubble plume distributions to evaluate methane hydrate decomposition on the continental slope, *Geochem. Geophys. Geosyst.*, *16*, 3825–3839, doi:10.1002/2015GC005955.

Received 30 JUN 2015
Accepted 28 SEP 2015
Accepted article online 1 OCT 2015
Published online 4 NOV 2015



# Analysis of bubble plume distributions to evaluate methane hydrate decomposition on the continental slope

**H. Paul Johnson[1], Una K. Miller[1], Marie S. Salmi[1], and Evan A. Solomon[1]**

[1]School of Oceanography, University of Washington, Seattle, Washington, USA

**Abstract** Cascadia margin sediments contain a rich reservoir of carbon derived both from terrestrial input and sea surface productivity. A portion of this carbon exists as solid gas hydrate within sediment pore spaces which previous studies have shown to be a methane reservoir of substantial size on both the Vancouver Island and Oregon portions of the Cascadia margin. Multichannel seismic reflection profiles on the Cascadia margin show the widespread presence of Bottom Simulating Reflectors (BSRs) within the sediment column, indicating the gas hydrate reservoir extends from the deformation front at 3000 m depth to the upper limit of gas hydrate stability near 500 m water depth. In this study, we compile an inventory of methane bubble plume sites on the Cascadia margin identified in investigations carried out for a range of interdisciplinary goals that also include sites volunteered by commercial fishermen. High plume density anomalies are associated with both the continental shelf (<180 m) and the depth of the upper limit of methane hydrate stability depth (MHSD) that occurs near 500 m in the NE Pacific. The observed anomalies on the Cascadia slope may be due to the warming of seawater at intermediate depths, suggesting that modern climate change has begun to destabilize the climate-sensitive hydrate reservoir within the Cascadia margin sediments. Reanalysis of similar plume images on the North American Atlantic slope suggests a lack of correlation between observed plume depths and the MHSD for much of the latitudinal range.

## 1. Introduction

Methane emissions from the decomposition of gas hydrate reservoirs on continental margins can play an important role in the regional marine environment. In Paleogene paleoclimate records, methane hydrate dissociation provided a powerful amplification factor to global warming that was initiated by massive volcanic eruptions in the Atlantic Basin [*Bowen et al*., 2015; *Wright and Schaller*, 2013]. During the Eocene, the massive release of methane from the sediment reservoir both decreased bottom water pH values [*Zachos et al*., 2005] and produced anoxia in the near-bottom water, which later propagated throughout the water column [*Sluijs et al*., 2006]. These paleoclimate studies suggest that modern climate warming due to anthropogenic greenhouse gas emission may also have a similar impact on the gas hydrate inventory present in modern margin sediments [*Bowen et al*., 2006]. *Hautala et al*. [2014] have recently demonstrated that the North Pacific Intermediate Water that bathes the upper slope of the Washington State continental margin has undergone a systematic warming of +0.3°C over the past 44 years. Thermal models of the propagation of heat from this warming trend into the sediments of Washington continental slope indicate that the methane hydrate stability depth (MHSD) has increased by 20 m vertically to its current depth at 500 m and moved seaward by more than 1 km over the past 4 decades. If *Hautala et al*. [2014] thermal model is correct, Washington margin sediments should presently be releasing methane gas into the water column preferentially at depths near the upper hydrate stability depth of 500 m, a hypothesis that is examined in the present study.

The accretionary wedge section of the Cascadia Subduction Zone (CSZ) in the NE Pacific Ocean extends along-strike for over 1000 km, from Cape Mendocino to central Vancouver Island. These accretionary margin sediments have been extensively studied due to the potential societal impact of a subduction megathrust earthquake on the populated coastal zone of western North America [*Hyndman et al*., 1993; *Hyndman*, 2013; *Atwater et al*., 2005; *Satake and Atwater*, 2007; *Goldfinger et al*., 2012; *Atwater et al*., 2014].

The upward migration of methane through Cascadia margin sediments has also been previously examined [*Ritger et al*., 1987; *Trehu et al*., 2004; *Riedel et al*., 2001, 2010; *Liu and Flemings*, 2006; *Riedel*, 2007;

*Daigle et al*., 2011]. Bottom Simulating Reflectors (BSRs) detected using multichannel seismic profiles indicate the presence of abundant solid methane hydrate and methane gas within the pore spaces of the upper several hundred meters of margin sediments. These reflector horizons have been identified as hydrates on the Oregon [*Torres et al*., 2009; *Trehu et al*., 2004, 2006; *Torres et al*., 2004; *Riedel et al*., 2006], Washington [*Booth-Rea et al*., 2008; *Holbrook et al*., 2012], and Vancouver Island [*Riedel et al*., 2006, 2010; *Malinverno et al*., 2008] continental slopes. Extensive authigenic carbonate surface accumulations related to the anaerobic oxidation of methane on the Cascadia margin, inferred from regions of high acoustic backscatter intensity, indicate that large-scale methane emissions have been active over geological time scales [*Carson et al*., 1994; *Torres et al*., 2009; *He et al*., 2007]. In addition, isotopic studies of foraminifera tests, bivalve shells and authigenic carbonate deposits of Pliocene age on the coastal Olympic Peninsula indicate that emissions have continued on this portion of the NE Pacific active margin for millions of years [*Martin et al*., 2007; *Nesbitt et al*., 2013].

On the Oregon and Vancouver Island portions of the Cascadia margin, methane bubble plume emission has been observed and studied over the last decade [*Orange et al*., 1997; *Suess et al*., 1999; *Torres et al*., 2004, 2009; *Trehu et al*., 2004, 2006; *Riedel et al*., 2006], with similar studies on the Washington margin [*Booth-Rea et al*., 2009; *Holbrook et al*., 2012]. Hydrate Ridge, a site of active methane plumes and shallow hydrate outcrops, has been the focus of multiple seismic surveys, several Deep Sea Drilling Project and Ocean Drilling Program drill holes, acoustic surveys of bubble plume emissions, and submersible programs, and is the site of an Ocean Observatories Initiative cabled observatory [*Suess et al*., 1999; *Torres et al*., 2002; *Bangs et al*., 2005, 2011; *Heeschen et al*., 2003, 2005; *Trehu et al*., 2004, 2006; *Bohrmann et al*., 2007; *Crutchley et al*., 2013]. Similarly, three active methane plume sites off the western margin of Vancouver Island have been well-studied [*Chapman et al*., 2004; *Riedel et al*., 2001, 2006, 2010; *Riedel*, 2007]. Although fewer in number than on the Oregon and Washington segments of Cascadia, the Vancouver Island methane emission sites have also been the site of ODP and IODP drilling and are a node of the Canadian NEPTUNE fiber optic cable network [*Barnes et al*., 2008; *Heesemann et al*., 2013]. Both the Vancouver Island and Hydrate Ridge sites are all located deeper than 600 m water depth, where gas emissions are not likely to be the result of modern seawater warming at midslope depths.

On the Washington margin, previous acoustic signatures of methane flux have detected regions of extensive seafloor surface carbonate deposits [*Salmi et al*., 2011]. Located on the continental shelf at 130 m water depth, these methane emissions are too shallow to be related to contemporary hydrate decomposition. Recent Remotely Operated Vehicle (ROV) and ship-based surveys on the deeper part of the Grays Harbor portion of the Washington margin have also detected large-scale seafloor carbonate deposits associated with long-term methane emissions, as well as water column methane gas plumes [*Johnson et al*., 2013] and prevalent BSRs in the subsurface [*Holbrook et al*., 2012]. During a 2013 heat flow survey of the Washington margin using the ROV Jason II and the R/V Atlantis, methane plumes at water depths of 1046 and 1988 m were discovered proximal to active bioherms [*Johnson et al*., 2013]. However, these deeper bubble plume emission sites lie significantly below the upslope hydrate decomposition depth. For this study, we characterize methane emissions over the entire depth range of the Cascadia margin, including at the upper limit of methane hydrate stability. The calculated upper feather edge of hydrate stability of $500 \pm 4$ m for the Washington margin is taken from the *Hautala et al*. [2014] study, and is reported as deeper at the south and shallower at the north end of the margin. The upper stability depth at the northern Oregon margin has been reported to be $\sim$510 m by other studies focused on the Hydrate Ridge region [*Torres et al*., 2009; *Bangs et al*., 2011; *Kannberg et al*., 2013].

## 2. Identification of Methane Plume Sites

Active methane gas emissions are detected through acoustic observations of bubble plumes in the water column (Figure 1 and supporting information Figure S1). These acoustic reflectors are oriented vertically in the water column, have a characteristic plume-like shape, are often referred to as flares, and appear to be sourced directly from the seafloor. Although diameters of the individual gas bubbles with a size distribution centered at approximately 2–4 mm [*Leifer and Culling*, 2010; *Römer et al*., 2012a; *Schneider von Deimling et al*., 2011] are too small to be individually reflected by sonar acoustic frequencies, which have wavelengths of tens of centimeters [*Salmi et al*., 2011], the collective groups of rising bubble streams and associated entrained bottom water present the strong impedance contrast required to acoustically image in the water

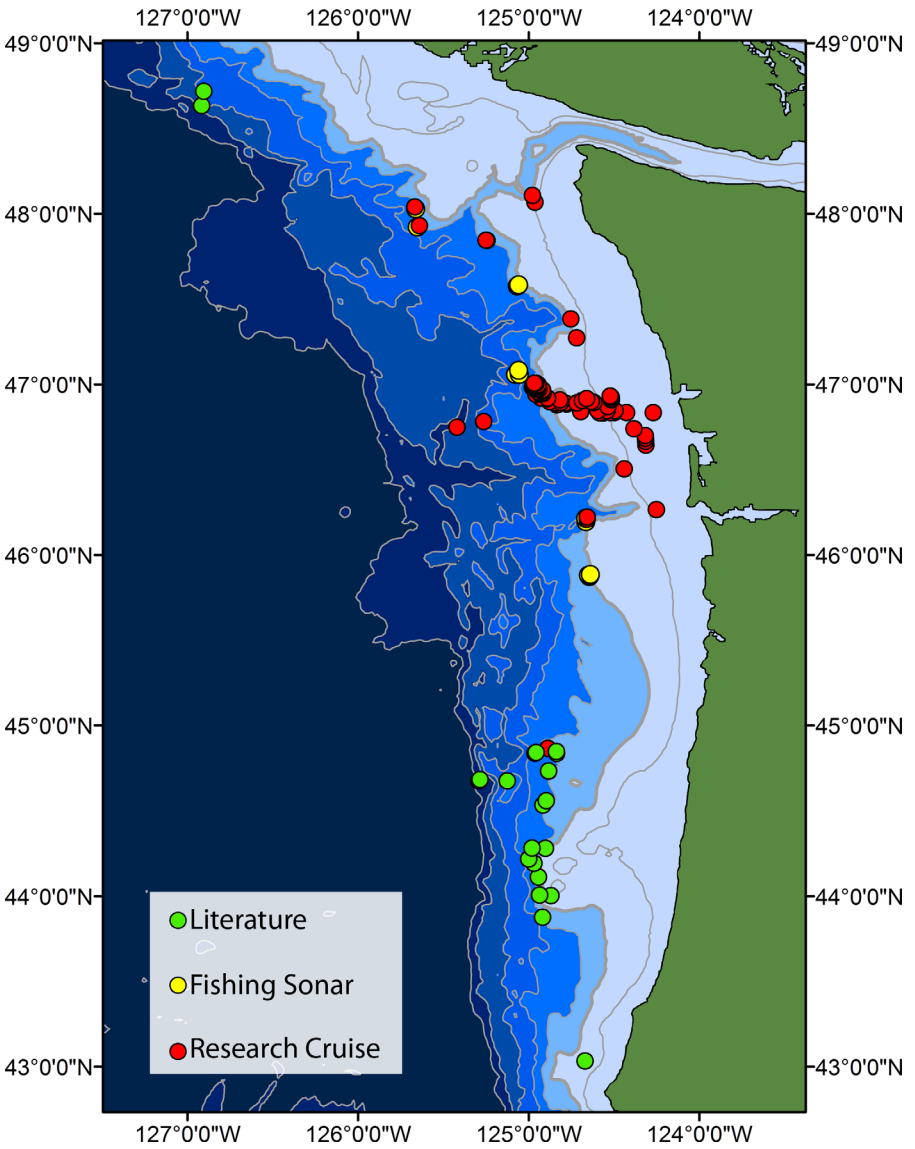


**Figure 1.** Methane emission sites on Cascadia Margin. Color of circles by data source. Red dots are sites from R/V Thompson and R/V Atlantis multibeam bathymetry surveys. Yellow dots are from reported fishing boat sonars. Green sites are taken from published literature. Total number of methane bubble streams (without clustering) is 168.

column (supporting information Figure S1) [*Leifer and Patro*, 2002; *Greinert et al*., 2006; *Römer et al*., 2012b; *Schneider von Deimling and Papenberg*, 2012; *Salmi et al*., 2011]., The installation of EM302 and EM122 Kongsberg swath bathymetry systems on the ships of the U.S academic research fleet have made it possible to routinely detect gas bubble plumes within the water column. These plume-like acoustic images have been confirmed as bubble streams using colocated ROV video images at a variety of sites [see *Torres et al*., 2009; *Salmi et al*., 2011; *Riedel*, 2007 for Cascadia examples] and have been used extensively as an indicator of bubble plumes in other continental margin environments [*Greinert et al*., 2006; *Greinert and McGinnis*, 2009; *Sauter et al*., 2006; *Römer et al*., 2012a; *Brothers et al*., 2013; *Skarke et al*., 2014]., Bubble plumes are also routinely detected by commercial fishing vessels, where sonar chirp frequencies range from 50 to 200 kHz, depending on the water depth and required resolution.

A major uncertainty associated with any compilation of methane emissions on global continental margins is the caveat that the bubble streams are discontinuous in both space and time [*Leifer et al*., 2006; *Greinert*, 2008; *Schneider von Deimling et al*., 2010]. Some emission sites, at all depths, are long-lived and surrounded by large associated carbonate deposits that take thousands of years to form [*Bayon et al*., 2009;

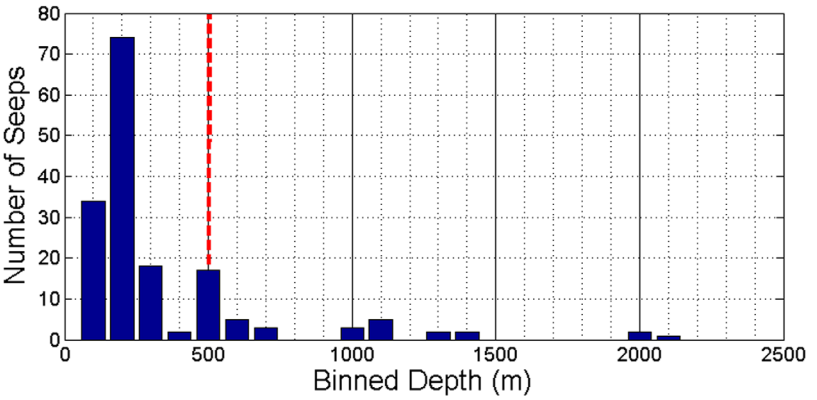


**Figure 2.** Histogram of all individual methane bubble streams observed in this study plotted as a function of site depth (m), with no clustering or normalization by area applied. Depth bins are 100 m wide, beginning at 50 m water depth. Note the strong peak in the 150–249 m depth bin where listric faults are present on the continental shelf edge between 150 and 249 m water depth.

*Berndt et al*., 2014; *Teichert et al*., 2003]. Methane emissions can be intermittent over a wide range of time scales [*Riedel*, 2007; *Bangs et al*., 2011; *Greinert and McGinnis*, 2009; *Kannberg et al*., 2013]. Where bubble plume emissions are episodic, they can sometimes be correlated with external tidal cycles or bottom water velocities [*Suess et al*., 2001; *Thomsen et al*., 2012]. In time series observations taken at methane emission sites, the bubble stream flows can appear randomly intermittent, with flow controlled by modifications such as blockage of subsurface pathways by gas accumulation or mineral precipitation processes not readily visible to seafloor or shipboard-based sensors [*Tryon et al*., 2002; *Solomon et al*., 2008; *Lapham et al*., 2013]. Because of obvious limitations on logistics and resources, we ignore any potential temporal variations and make the simplistic assumption that the plume distributions are static and constant, at least over the past 10 years of data acquisition.

The 168 active methane gas emission sites in this study were compiled from both traditional and nontraditional sources (Figures 2 and 3). Most sites were discovered in the course of systematic geophysical surveys of relatively small areas of the margin. Many but not all of the bubble streams were later confirmed as methane gas by surface ship CTD casts, and submersible ALVIN and ROV water sampling. The majority of the methane plume sites identified on the Oregon portion of the Cascadia margin are from the compilation of *Torres et al*. [2009] using these methods. Three well-studied methane plume sites off the west coast of Vancouver Island are of a similar nature and are described in *Riedel et al*. [2010, and references within].

Included in the present compilation are 45 bubble plumes discovered and informally contributed by commercial fishermen using standard deep water acoustic fish locating sonars. Modern commercial fish locating sonars are integrated with GPS navigation that can provide colocated seafloor depths, surface ship GPS location, and images of plume-like reflectors in the water column. The photographic images of these reflectors were recorded by commercial fishermen using cell phone cameras, and were provided to the authors over a period of several years (Figure 3a and supporting information Figure S1). An important subset of the plume sites detected by fisherman was later confirmed by subsequent scientific field programs using swath bathymetry and water column imaging of the EM302 system on the R/V Thomas G. Thompson.

For the acoustic images obtained with fishing and other research vessel sonars to be identified as methane plumes, these reflectors were required to (1) be oriented subvertically, (2) extend at least 50 m upward through the water column, (3) clearly originate at the seafloor, and (4) not match the criteria used to identify fish or other biological swarms including acoustic reflection lobes that spread horizontally at a given water depth (supporting information Figure S1).

An issue in interpreting the present compilation is the confirmation that acoustically imaged bubble plumes are actually composed solely of pure methane gas of microbial origin rather than a more complex organic gas of thermogenic origin, which would push the upper limit of gas hydrate stability to shallower depths. *Torres et al*. [2009] and *Collier and Lilley* [2005] show that most of the methane plumes in the Oregon margin compilation are composed primarily of methane gas, with only minor amounts of heavier hydrocarbons. These and other studies showed that many of the bubble streams off the Oregon coast are associated with

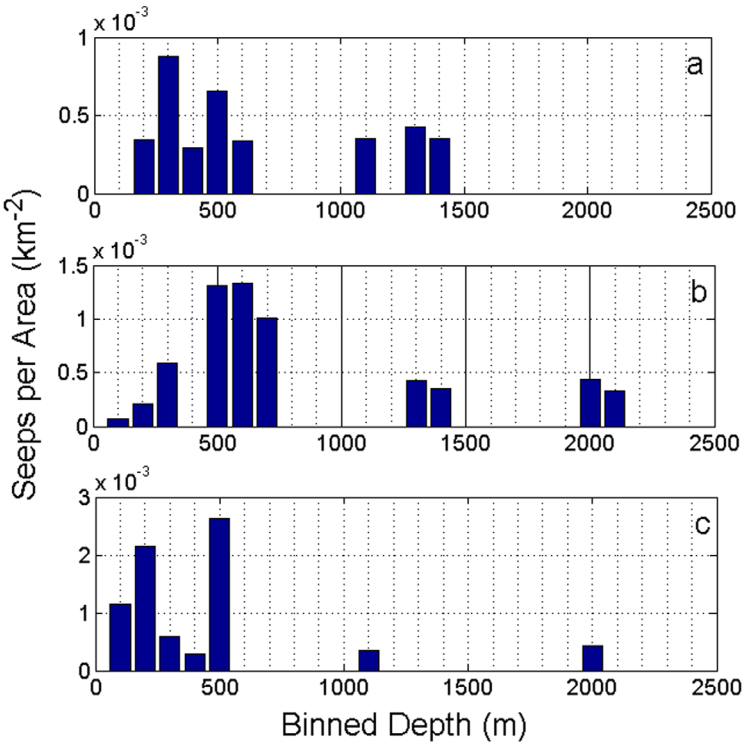


**Figure 3.** (a) Methane plumes identified using fishing sonars that have been normalized by area of depth bins and clustered using 300 m radii. (b) Methane plume sites taken from scientific literature normalized by area of depth bin and clustered using 300 m radii. (c) Methane plume sites taken from University of Washington research cruises on the R/V Thomas G. Thomson and R/V Atlantis and normalized by the area of each depth bin and clustered using 300 m radii.

surface exposures of solid methane hydrate [*Johnson et al*., 2003; *Kannberg et al*., 2013, and references within]. However, many Oregon margin sites are located deeper than the upper limit of hydrate stability (Figure 4) and therefore unlikely to be derived from the decomposition of hydrate by contemporary warming of near-bottom seawater. The plume sites on the Vancouver Island segment of the Cascadia margin, also located below the hydrate stability depth, have been confirmed to be composed of both microbial and thermogenic methane gas, are associated with seafloor exposures of solid gas hydrate, and are proximal to extensive long-lived seafloor carbonate deposits [*Riedel et al*., 2010; *Joseph et al*., 2013; *Lapham et al*., 2013].

## 3. Depth Determination

Of the 168 total bubble stream emission sites, 103 sites have water depths extracted from the original fishing or research vessel acoustic sounder data, using the travel time of the acoustic return. These travel time depths could range in confidence from the fixed acoustic velocity values used for fishing sonars to the CTD-calibrated depths used during the research cruises. Each of these depths was tested by colocating the methane emission site with a Cascadia Margin multibeam bathymetry compilation within GeoMapApp (http://www.geomapapp.org) and comparing it to the depth provided by this bathymetric data. Of the 103 total sites compared using primary source depths and GeoMapApp depth, 77 locations agreed within 10 m and 90 locations agreed within 50 m. The GeoMapApp multiple resolution depth compilation includes both modern high-resolution swath bathymetry that overlies a lower resolution NOAA multibeam bathymetry data set [*Ryan et al*., 2009]. Three of the sites exceeded 100 m depth disparity between reported primary source depths and GeoMapApp depths, but these corresponded to the low-resolution portions of the compiled bathymetric data. Depths provided by the primary reporting sources were used in all calculations in the study where available. However, 65 of the total 168 sites had only locations without original reported depths and their depths were taken from the GeoMapApp bathymetric compilation. Supporting information Figure S4 compares primary source depths with those depths given at the same location by the

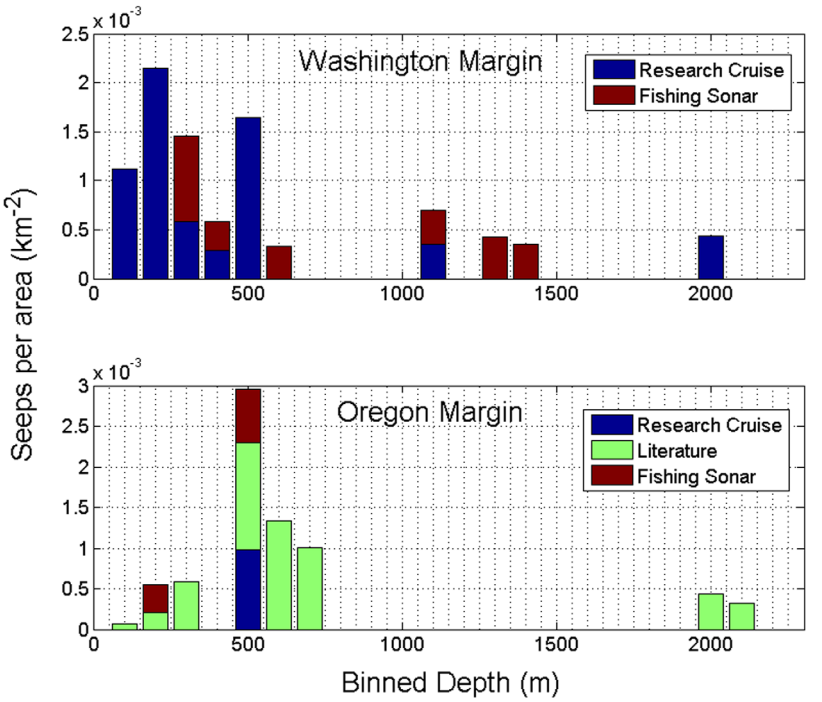


**Figure 4.** North-South geographic partitioning of methane plume sites, all with a clustering of 300 m for individual bubble streams applied to the data and normalized by area for each 100 m depth bin. (top) Data from the WA margin between the Straits of Juan de Fuca to the Columbia River. (bottom) Data from the OR margin between the Columbia River and the California state line. For both of these North-South segments of the Cascadia margin, the depth bins that include 500 m water depth that are normalized by area have a high density of methane emission sites shown as peaks in the respective histograms.

GeoMappApp bathymetry data. The high correlation lends confidence to the use of GeoMapApp depths where depth data are otherwise absent.

There are general increasing uncertainties associated with each of these depth assignments, where depths derived from submersible or ROV observations are assumed accurate within several meters. Depths from the R/V Thompson EM302 coverage have estimated accuracies of $\pm 5$ m, largely due to uncertainties in the horizontal positioning of the ship, and those depths from fishing sonars were assigned an uncertainty of $\pm 10$ m due to the use of fixed factory-calibrated water velocity profiles. The uncertainties were estimated by comparing site depths obtained from GeoMapApp using the latitude and longitude of the site locations to those original reported depths taken from research cruises, literature, and fishing sonar images where there was overlap in coverage for the same bubble plume locations (supporting information Figure S4).

## 4. Data Processing

### 4.1. Bubble Stream Clustering

Areas of methane emissions can consist of multiple individual gas streams that are partitioned in the shallow subsurface just prior to entering the water column. As an example, a detailed survey of an emission site located on the Washington continental shelf shows approximately 20 individual bubble streams rising within the water column originating from what appears to be a single deeper subsurface source of methane [*Salmi et al.*, 2011, Figure 1]. In order to not overestimate sites composed of multiple but closely related bubble streams, individual bubble plumes were grouped together in order to identify bubble streams that share a common subsurface pathway. We applied a clustering strategy that consolidates all gas streams located within a fixed radius of 300 m, using the well-characterized *Salmi et al.* [2011] site as our guide. A similar distribution of individual methane gas streams is present on the Vancouver Island Barkley Canyon site, although the collection radius used there is somewhat larger than the 300 m radius selected for this compilation [see *Riedel*, 2007]. Some methane emission sites, particularly the quasi-linear distribution visible

on the Washington shelf near Grays Canyon (Figure 1) appear controlled by listric fault traces that are not point sources [*McNeill et al*., 1997] and are therefore unlikely to have a characteristic clustering radius.

To reiterate the clustering process, if there were distinct bubble streams identified within a clustering radius of 300 m, they were still counted in this compilation as only one emission site. This process reduced the number of plumes from 168 to 113. We arrived at a standard radius of 300 m by testing clustered radii of 0, 150, 300, and 500 m, to identify a characteristic length scale for emission sites where the number of total sites counted would become almost constant with increasing radii. Supporting information Figure S3 shows the number of plumes sites flattening with increasing clustering radii between 300 and 500 m, suggesting that 300 m is approaching but not yet reaching the full characteristic length scale for methane emission sites on the Cascadia margin.

### 4.2. Areal Normalization

The Cascadia margin is an active accretionary wedge where the bathymetric depth varies nonuniformly both across-strike and along-strike of the subduction zone convergence. This variation produces significant differences in the amount of area associated with each across-strike depth interval of the margin (supporting information Figure S2). For example, the entire Cascadia margin continental shelf between the depths of 50 and 149 m has an area of $2.68 \times 10^4$ km$^2$, while the depth interval over the same 100 m spacing between 450 and 549 m has a much smaller surface area of $3.41 \times 10^3$ km$^2$. Without areal normalization, a uniform distribution of emission sites should produce a higher bubble stream count for depth intervals that have the largest exposed horizontal area, such as the continental shelf margin and midslope terraces which have larger horizontal areas. In order to compare methane plume density across depth intervals of varying areas, we normalized the observed plume density to area by using the following equation:

$$\text{Normalized plume density at } D = N_p/(A)$$

where $N_p$ is the plume site count, A is the area associated with each 100 m depth interval along the entire margin, and D specifies the depth interval in meters (i.e., normalized plume density in plumes/km$^2$ for a specific 100 m wide depth bin, D).

Areal normalization provides a more accurate measure of bubble stream density with units of plumes/km$^2$ per depth interval than simple depth binning methods that have been used previously. For this normalization, we used the compiled margin bathymetry data set available for Cascadia in GeoMapApp, subdivided the margin depths into 100 m depth bins for each of the depth intervals on the Cascadia margin (i.e., 50–149, 150–249, 250–349, . . ., in m). We then calculated the areas for each depth interval using the geospatial processing program ArcMap. Plume densities are discussed in terms of these area-normalized units for the remainder of this report.

### 4.3. Nonuniform Sampling Bias

Non-uniform and incomplete sampling of the entire Cascadia margin can produce bias in a compilation of ad hoc emission sites. No complete systematic geophysical survey of methane emission sites of the entire Cascadia margin presently exists, although *Torres et al*. [2009] have compiled many sites within a compact region of the Oregon coast near Hydrate Ridge, and the Grays Canyon area of Washington State has also had considerable coverage over a small area [*Holbrook et al*., 2012; *Johnson et al*., 2013]. Scientific expeditions with goals other than methane bubble stream identification are nonuniformly distributed along the Cascadia margin, with many located at water depths deeper than the 500 m upper limit of the MHSD for Cascadia. While useful in characterizing acoustic images associated with bubble streams and for confirming those from fishing sonar anomalies, these focused scientific research expeditions have primarily targeted localized areas on the midslope and lower slope of the Cascadia margin and do not provide uniform areal coverage.

Any bias toward midslope to upper slope depths by fishing sonar surveys on the Cascadia margin is difficult to quantify, since there is no estimate available of the time each fishing boat spends surveying at each depth interval. Fish catch reports indicate that the most completely sampled regions by the Cascadia margin commercial fishing fleet are the upper slope above 1000 m depth (http://www.nwfsc.noaa.gov/research/divisions/fram/observation/data_products/index.cfm). The incomplete and nonuniformly sampled margin coverage for all data sources will limit confidence in any interpretation of our compilation, which

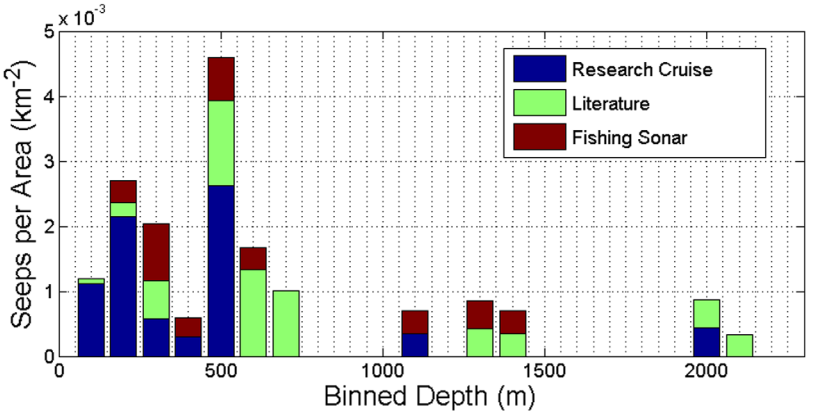


**Figure 5.** Histogram showing all methane emission sites on the Washington and Oregon segments of the Cascadia margin, with 300 m clustering applied to the individual bubble streams and normalized by the area contained within each 100 m depth bin. Color bar legend shows methane plume site data sources.

must be viewed critically in this light. Since the primary hypothesis being tested is whether or not methane bubble plumes on the Cascadia margin have an unusual density in the range of depths that includes the upper limit of gas hydrate stability, an ideal compilation producing Figure 5 would require that all Cascadia continental slope depths would have been surveyed uniformly using a single methodology. Given the ad hoc and informal sources of some plume identifications in our compilation, this desired uniformity and completeness of spatial coverage is clearly not realized, and is further discussed below.

### 4.4. Sensitivity Tests

We performed a series of sensitivity tests to test confidence in our interpretations based on the observed methane bubble plumes from this compilation. The first test is whether the anomalous plume densities shown in Figure 5 are due to only one of the data sources for the compilation, or are present independently in all three of the source subdata sets. Figures 3a–3c show the partitioning of the plume depth inventory by source, differentiating between plumes exclusively from fishing sonars, those from research cruises and those from published ROV and submersible studies. Examination of these histograms shows that a peak in plumes/km$^2$ at the depth bin for 500 (i.e., 450–549) m is present in all subsets of the compilation (supporting information Figure S4), and is not dependent on the source of the identifications.

The plume density anomaly was also tested for along-strike geographical bias. Figure 4 shows plume distributions divided geographically into Washington and Oregon portions of the Cascadia margin. This figure indicates that the plume sites for both geographic areas show an unusually high density of emission sites in the 500 m depth interval that is associated with the upper hydrate stability depth. Figure 4 also shows that most of the Oregon emission sites are derived from published research expeditions rather than more recent fishing sonar observations. In contrast, the plume densities on the Washington segment have a broader mix of sources that include fishing sonar, R/V Thompson and R/V Atlantis cruises, and published methane plume sites (Figure 4). Even though the Washington and Oregon segments have a widely different mix of plume identification sources, comparison of the two geographical regions both show an anomalously high plume density near 500 m water depths.

## 5. Anomalous Bubble Plume Density for Cascadia

Using our preferred bubble stream clustering radius of 300 m, Figure 5 represents our estimate of the depth distribution of the 113 methane plume sites detected by the data acquisition methods described above. The original large plume depth anomaly at the depths of less than 200 m for unclustered individual bubble streams for the shallow continental shelf in Figure 2 is reduced by applying the clustering process. Significantly, the peak plume density anomaly at the 500 m depth interval persists after clustering. Of the total clustered 113 emission sites in this collection for the entire Cascadia margin at all depths, 14 sites lie within the narrow 450–549 m depth range, which includes the upper hydrate stability depth of 500 m.

## 6. Thermal Penetration Depth

A recent study of the in situ thermal diffusivity of Cascadia margin sediments allows quantitative estimates for the penetration depth of water column temperature changes. Using an experimentally determined thermal diffusivity of $4.33 \times 10^{-7}$ $m^2$ $s^{-1}$ for margin surface sediments, *Homola et al.* [2015] calculate thermal penetration depths of 4, 12, and 23 m for intervals of 1, 10, and 40 years, respectively. However, thermal diffusion into a conducting infinite half-space is the slowest method of propagation for water column temperature changes, and rough surface topography, the presence of faults and shallow fluid circulation cells in high porosity turbidites can extend these depths by an order of magnitude [*Henry et al*., 1996; *Tryon et al*., 2002; *Solomon et al*., 2008].

## 7. Discussion and Interpretation

We approached this study with the goal of addressing the specific question: are there any plume density anomalies located across-strike the Cascadia Margin? If these density anomalies exist, are they located within the depth interval that contains the upper limit of hydrate stability? Logically, there are three possible alternative plume distributions that form the corresponding Null Hypotheses to this question. The first Null Hypothesis is that methane plume sites might have a uniform depth distribution along the Cascadia margin. However, even without the application of any filters, the bubble stream distributions shown in Figures 2 and 5 indicate that this Null Hypothesis is unlikely to be correct.

The second Null hypothesis is that any observed nonuniform distribution of methane emissions with depth would be controlled by tectonic and geological processes that are unrelated to changing seawater temperatures or hydrate decomposition and instead are controlled by subsurface tectonic and biogeochemical processes present. Figures 2 and 5 show a very nonuniform distribution for the bubble emission sites, with plume density anomalies associated with both the continental shelf (<200 m) and the depth of the upper limit of hydrate stability at 500 m. In shallow water, the Washington continental shelf edge has been previously shown to be an extensional region with deep listric faults [*McNeill et al*., 1997**]**, and these fault traces are sites of both fluid and methane emissions [*Salmi et al*., 2011].

It is important to note that there are drivers of fluid and gas emissions other than hydrate decomposition within an accretionary wedge, including sediment compression at the deformation front and compaction with depth and dehydration of clay minerals within the warm, accumulating sediment pile. Both highly permeable turbidites and deeply penetrating faults can deliver this fluid and gas to the seafloor at all depths as the margin evolves, including to the MHSD and shallow continental shelf depths. Previous tectonic models of fluid and gas migration for an active accretionary wedge predict observed plume emissions occurring near 2000 m, 1000 m, and on the shallow continental shelf region. In these models, the deeper sites near 2000 m have been suggested to be due to sediment porosity reduction directly behind the deformation front [*Hyndman et al*., 1993; *Wang et al*., 1993; *Wang*, 1994; *Shi and Wang*, 1994; *Riedel et al*., 2010]. In addition, the fluid/gas emissions occurring near 1000 m depths have been proposed to be due to the development of late stage tectonic fault pathways that penetrate deeply into the middle portion of the accretionary sediment wedge [*Wang et al*., 1993; *Moore et al*., 1991; *Moore and Vrolijk*, 1992; *MacKay et al*., 1992; *Davie and Buffett*, 2003; *Bangs et al*., 2011; *Mandal et al*., 2014; *Hornbach et al*., 2012; *Li et al*., 2014; *Saffer*, 2014]. In contrast to this model, observations using acoustic backscatter images of seafloor carbonate deposits suggest that the subsurface fluid/methane vertical migration paths are strongly correlated with, and the locations primarily controlled by, the development of folded anticlinal ridges associated with the horizontal shortening of the accretionary wedge [*Carson et al*., 1991, 1994, *Johnson et al*., 2003].

In regard to the critical minimum depth of gas hydrate stability near 500 m in the North Pacific, we are not aware of any tectonic model that predicts a higher density of methane emission sites either below the shelf edge at 200 m or above the near-1000 m depth interval. However, we note that the lack of a currently published model does not indicate the absence of a yet-undescribed tectonic process. The model of *Hautala et al*. [2014] requires that bubble plumes be present at the MHDS, and at perhaps a higher density than is present over the remainder of the margin, since hydrate decomposition does not occur at other depths. However, the simple presence of the plume density anomaly, as shown by our limited data, does not prove the case for hydrate decomposition due to water column warming, but does make the hypothesis very plausible.

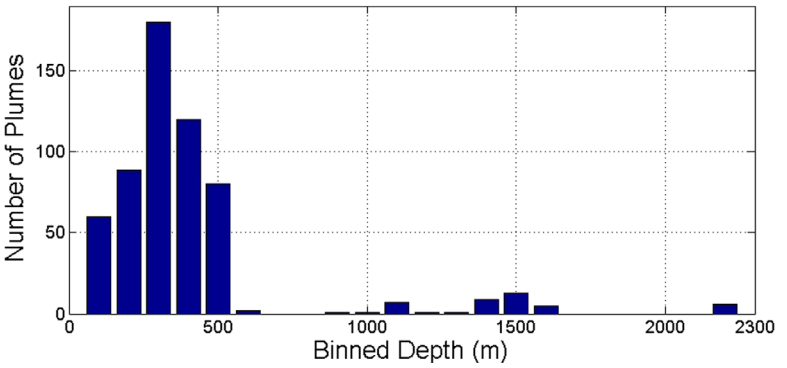


**Figure 6.** Histogram of methane plumes on the Atlantic margin taken from *Skarke et al*. [2014, supporting information] compilation, but with application of the same clustering radii of 300 m as used on the Cascadia margin in Figures 3–5 for the Cascadia sites within this compilation. No area normalization was applied to this data.

The third possible Null Hypothesis is that if our plume compilation shows an anomalously high emission site density within the depth range that contains the upper hydrate stability depth of 500 m, this density anomaly could still be solely the result of areal/depth sampling biases from incomplete survey coverage of the entire continental slope. Due to the ad hoc nature of our plume site sources, our data compilation may be fundamentally biased by spatially nonuniform survey track lines that cannot be addressed quantitatively. Although difficult to verify, we assume that the fishing sonar observations of methane plumes may be more frequent on the shelf and upper margin midslope to 1000 m water depth. In contrast, subduction zone-related research cruises and resultant emission sites taken from the reviewed scientific literature are likely to be surveying the lower midslope and deformation front on the deep margin rise. These opposing depth/spatial biases could partially compensate for the commercial fishing sonar observations, although this hopeful assumption may not be supported by more systematic geophysical surveys in the future.

## 8. Results From Cascadia Margin

Whether partitioned by (1) bubble stream cluster radius, (2) plume identification method, (3) geographical region, or (4) normalized for the area of each depth interval on the entire margin, the narrow 100 m wide depth range that includes upper hydrate stability depth of 500 m on the Cascadia margin appears to be an anomalously active region of methane plume emissions. Lacking any known alternative tectonic or geologic model that would produce anomalously high number of emission sites in this narrow depth range, and with new evidence that 44 years of seawater warming is also occurring at this depth, a plausible remaining explanation is that methane hydrates at the upslope feather edge of phase stability appear to be decomposing along the entire Cascadia margin.

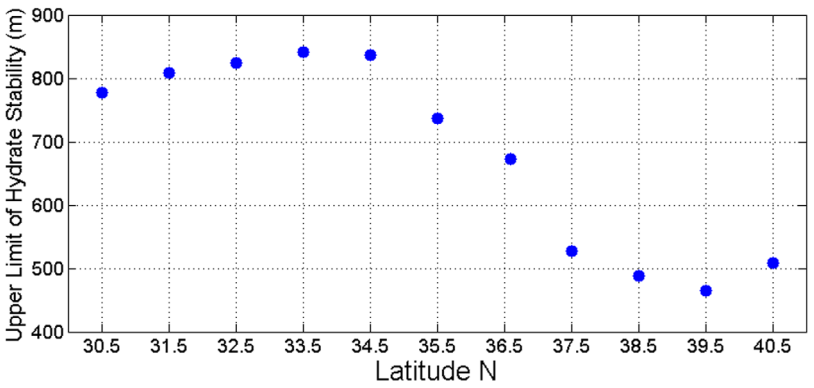


**Figure 7.** Plot of the upper methane hydrate stability depth for the U.S. Atlantic sea coast as a function of latitude along that margin. Comparison of this figure, supporting information Figure S5, and supporting information Table S1 suggests that only plumes imaged north of 36.5 N are near the upper limit of the methane hydrate stability zone, and plumes imaged to the south may not be related to recent seawater warming.

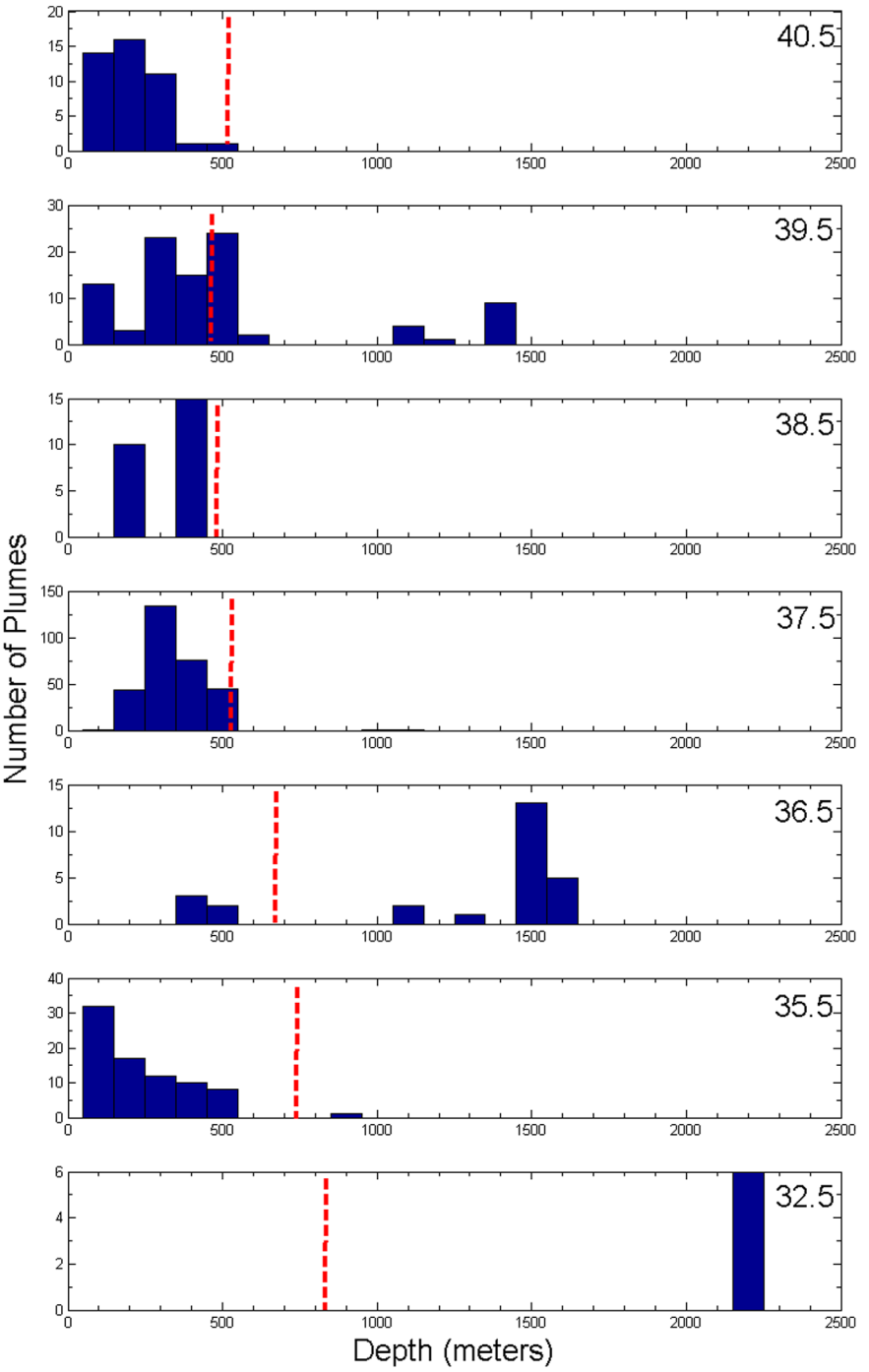


**Figure 8.** Partitioning of the methane plume emission sites taken from *Skarke et al*. [2014, supporting information]. Site locations were divided by 1° of latitude, from 41°N to 30°N, with locations shown in Table S1 in the supporting information. For comparison with Cascadia margin data, emission sites for this Atlantic Figure are binned in 100 m depth bins, similar to Figures 2–5 in the main text. Dashed red lines are the calculated MHSD depths for the same latitudinal partitions for the Atlantic margin in *Skarke et al*. [2014] and shown in Table S1 in the supporting information. Note that 100 m bins centered on 34.5°, 33.5°, 31.5°, and 30.5° North latitude are not shown, as the *Skarke et al*. [2014] compilation did not list any methane emissions in those latitudes. No clustering or areal normalization was applied to the data for this figure.

This proposed hypothesis is consistent with a previous thermal model of the Cascadia upper continental slope that shows gas hydrates may have begun to dissociate in response to seawater warming observed in this depth interval and at this location [*Hautala et al*., 2014]. That previous study used archived water temperature

profiles to show that seawater in the Washington segment of Cascadia in the interval 400–700 m has risen +0.007°C/yr over the past 45 years. Depending on local margin bathymetry, this warming is sufficient to cause the upper methane hydrate stability depth to migrate vertically 10–20 m over this time period, releasing substantial quantities of methane gas [*Hautala et al*., 2014]. If our assumptions and analyses are correct, the unusual density of methane plume emission sites at the upper stability limit for methane hydrate shown in Figure 5 is consistent with thermal models that show contemporaneously warming seawater is causing hydrates to decompose along the entire Cascadia margin, potentially from Northern California to Vancouver Island. While the above argument is plausible, it falls short of providing the confidence level that a uniform survey of the entire Cascadia margin, optimally using a single survey tool, would provide.

## 9. Comparison to the North American Atlantic Margin

Recent studies have also suggested extensive methane hydrate decomposition due to warming seawater on the mid-Atlantic margin of North America (Figure 6) [*Phrampus and Hornbach*, 2012; *Brothers et al*., 2013; *Skarke et al*., 2014] and in the Beaufort Sea [*Phrampus et al*., 2014]. For the Cascadia margin, the upper MHSD varies by only 4 m over the latitude range from 48°N to 46.5°N and 13 m from the Juan de Fuca Canyon to Hydrate Ridge [*Hautala et al*., 2014]. However, the diverse water temperatures of the Atlantic margin produce a much wider range of MHSD depths, from 850 to 450 m (Figure 7 and supporting information Figure S5a). In contrast to the Cascadia margin where the anomalous plume density corresponds to the MHSD, the depths of the abundant methane plumes visible in the water column imagery for the U.S. Atlantic plume sites presented in *Skarke et al*. [2014] do not correspond everywhere with upper feather-edge hydrate stability depth (Figure 8 and supporting information S5a, Methods) [*Skarke et al*., 2014; *Brothers et al*., 2013]. Without additional data and systematic surveys of plume areal densities and local seawater properties, and consideration of the latitudinal variation in the upper limit of hydrate stability, the full extent of widespread contemporary methane hydrate decomposition on all North American continental margins still remains an important open question.

## 10. Conclusions

The present compilation of methane emission site densities along the Cascadia margin in the NE Pacific suggests that methane emission sites are preferentially located within depths represented by both the continental shelf and at the 500 m depth on the margin, with the latter representing the depth interval that contains the upper limit of gas hydrate stability. However, this compilation includes nontraditional data acquisition methods and lacks the weight of a systematic geophysical survey with 100% areal coverage. The number of plumes within the 450–549 m depth bin represents only 12% of the total emission sites from all depths over the entire Cascadia margin, and is considerably smaller than the 67% of emission sites previously considered derived from hydrate decomposition on the upper slope of the Atlantic margin [*Skarke et al*., 2014]. However, along the U.S. Atlantic margin plume emissions only directly correlate with the upper limit of the methane hydrate stability zone north of 37.5°N (supporting information Figure S5), limiting the number of identified seep sites related to methane hydrate dissociation along the U.S. east coast.

The area normalization for each of the 100 m Cascadia depth bins and the persistence of the resulting emission peak at 500 m after the application of several sensitivity tests adds weight to our proposed identification of the 14 emission sites as a substantial depth anomaly for methane emissions. Given this anomalous density of methane emission sites at the critical hydrate decomposition depth, the present Cascadia compilation is consistent with thermal models that show the observed warming of North Pacific seawater over the past several decades. This warming may be decomposing the previously stable hydrate reservoir along the entire Cascadia Margin [*Hautala et al*., 2014]. If this hypothesis is correct, extensive decomposition of methane hydrate on the active Cascadia margin sediments has potential for major societal impact, including changes in near-bottom seawater chemistry including oxygen consumption and ocean acidification (pH) anomalies harmful to local near-bottom dwelling biota, possible tsunami-generating slope failures, and a potential positive feedback to atmospheric greenhouse gas emissions.

Extracting useful information from imperfect data sets has a strong tradition in oceanography, and with proper caveats, can be used to advance current models regarding critical processes to the next stage of

understanding. The way forward is obvious; a systematic geophysical and geochemical examination of the entire Cascadia continental margin as well as other active and passive margins is required that includes the entire depth range from the continental shelf to the abyssal plain.

**Acknowledgments**

Support was provided by NSF/GeoPRISM award 1339635 to H.P.J. and E.A.S. and Department of Energy award DE-FE0013998 to E.A.S. and H.P.J. We thank Brian Atwater, Marta Torres, Susan Hautala, and Emily Roland for useful reviews of this manuscript. We also thank Peter Lathourakis for his help in sending us plume locations from his fishing expeditions, which initiated this project. Excel files with the basic data for the Cascadia methane plumes used in this study (latitude, longitude, depth, identification source of plume sites) are available on the following UW public web site. https://catalyst.uw.edu/workspace/paulj/17643/372058. Also available on the same web site are Excel files with the basic data used to generate Figures 6–8 and supporting information Figure S5 and Table S1 for the U.S. Atlantic coast.

## References

Atwater, B. F., S. Musumi-Rokkaku, K. Satake, Y. Tsuji, K. Ueda, and D. K. Yamaguchi (2005), The Orphan Tsunami of 1700: Japanese clues to a parent earthquake in North America, *U.S. Geol. Surv. Prof. Pap., 1707*, 144 pp.

Atwater, B. F., B. Carson, G. B. Griggs, H. P. Johnson, and M. S. Salmi (2014), Rethinking turbidite paleoseismology along the Cascadia subduction zone, *Geology*, *42*(9), 827–830.

Bangs, N. L., M. J. Hornbach, and C. Berndt (2011), The mechanics of intermittent methane venting at South Hydrate Ridge inferred from 4D seismic surveying, *Earth Planet. Sci. Lett.*, *310*(1), 105–112.

Barnes, C. R., M. M. R. Best, and A. Zielinski (2008), The NEPTUNE Canada regional cabled ocean observatory, *Technology (Crayford, England) 50*, 3.

Bayon, G., G. M. Henderson, and M. Bohn (2009), U-Th stratigraphy of a cold seep carbonate crust, *Chem. Geol.*, *260*(1), 47–56.

Berndt, C., et al. (2014), Temporal constraints on hydrate-controlled methane seepage off Svalbard, *Science*, *343*(6168), 284–287.

Bohrmann, G., W. F. Kuhs, S. A. Klapp, K. S. Techmer, H. Klein, M. M. Murshed, and F. Abegg (2007), Appearance and preservation of natural gas hydrate from Hydrate Ridge sampled during ODP Leg 204 drilling, *Mar. Geol.*, *244*(1), 1–14.

Booth-Rea, G., D. Klaeschen, I. Grevemeyer, and T. Reston (2008), Heterogeneous deformation in the Cascadia convergent margin and its relation to thermal gradient (Washington, NW USA), *Tectonics*, *27*, TC4005, doi:10.1029/2007TC002209.

Bowen, G. J., et al. (2006), Eocene hyperthermal event offers insight into greenhouse warming, *Eos Trans. AGU*, *87*(17), 165–169.

Bowen, G. J., B. J. Maibauer, M. J. Kraus, U. Röhl, T. Westerhold, A. Steimke, P. D. Gingerich, S. L. Wing, and W. C. Clyde (2015), Two massive, rapid releases of carbon during the onset of the Palaeocene-Eocene thermal maximum, *Nat. Geosci.*, *8*(1), 44–47.

Brothers, L. L., C. L. Van Dover, C. R. German, C. L. Kaiser, D. R. Yoerger, C. D. Ruppel, E. Lobecker, A. D. Skarke, and J. K. S. Wagner (2013), Evidence for extensive methane venting on the southeastern US Atlantic margin, *Geology*, *41*(7), 807–810.

Carson, B., M. L. Holmes, K. Umstattd, J. C. Strasser, and H. P. Johnson (1991), Fluid expulsion from the Cascadia accretionary prism: Evidence from porosity distribution, direct measurements, and GLORIA Imagery, *Philos. Trans. R. Soc. London A*, *335*, 331–340.

Carson, B., E. Seke, V. Paskevich, and M. L. Holmes (1994), Fluid expulsion site on the Cascadia accretionary prism: Mapping diagenetic deposits with processed GLORIA imagery, *J. Geophys. Res.*, *99*(B6), 11,959–11,969.

Chapman, R., J. Pohlman, R. Coffin, J. Chanton, and L. Lapham (2004), Thermogenic gas hydrates in the northern Cascadia Margin, *Eos Trans. AGU*, *85*(38), 361–365.

Collier, R. W., and M. D. Lilley (2005), Composition of methane seeps on the Cascadia continental margin, *Geophys. Res. Lett.*, *32*, LO6609, doi:10.1029/2004GL022050.

Crutchley, G. J., C. Berndt, S. Geiger, D. Klaeschen, C. Papenberg, I. Klaucke, M. J. Hornbach, N. L. B. Bangs, and C. Maier (2013), Drivers of focused fluid flow and methane seepage at south Hydrate Ridge, offshore Oregon, USA, *Geology*, *41*(5), 551–554.

Daigle, H., N. L. Bangs, and B. Dugan (2011), Transient hydraulic fracturing and gas release in methane hydrate settings: A case study from southern Hydrate Ridge, *Geochem. Geophys. Geosyst.*, *12*, Q12022, doi:10.1029/2011GC003841.

Davie, M. K., and B. A. Buffett (2003), Sources of methane for marine gas hydrate: Inferences from a comparison of observations and numerical models, *Earth Planet. Sci. Lett.*, *206*(1), 51–63.

Goldfinger, C., et al. (2012), Turbidite event history—Methods and implications for Holocene paleoseismicity of the Cascadia subduction zone: *U.S., U.S. Geol. Surv. Prof. Pap., 1661-F*, 170 pp. [Available at http://pubs.usgs.gov/pp/pp1661f/.]

Greinert, J. (2008), Monitoring temporal variability of bubble release at seeps: The hydroacoustic swath system GasQuant, *J. Geophys. Res.*, *113*, C07048, doi:10.1029/2007JC004704.

Greinert, J., and D. F. McGinnis (2009), Single bubble dissolution model–The graphical user interface SiBu-GUI, *Environ. Modell. Software*, *24*(8), 1012–1013.

Greinert, J., Y. Artemov, V. Egorov, M. De Batist, and D. McGinnis (2006), 1300-m-high rising bubbles from mud volcanoes at 2080m in the Black Sea: Hydroacoustic characteristics and temporal variability, *Earth Planet. Sci. Lett.*, *244*(1), 1–15.

Hautala, S. L., E. A. Solomon, H. P. Johnson, R. N. Harris, and U. K. Miller (2014), Dissociation of Cascadia margin gas hydrates in response to contemporary ocean warming, *Geophys. Res. Lett.*, *41*(23), 8486–8494, doi:10.1002/2014GL061606.

He, T., G. D. Spence, M. Riedel, R. D. Hyndman, and N. R. Chapman (2007), Fluid flow and origin of a carbonate mound offshore Vancouver Island: Seismic and heat flow constraints, *Mar. Geol.*, *239*(1), 83–98.

Heeschen, K. U., A. M. Tréhu, R. W. Collier, E. Suess, and G. Rehder (2003), Distribution and height of methane bubble plumes on the Cascadia Margin characterized by acoustic imaging, *Geophys. Res. Lett.*, *30*(12), 1643, doi:10.1029/2003GL016974.

Heeschen, K. U., R. W. Collier, M. A. de Angelis, E. Suess, G. Rehder, P. Linke, and G. P. Klinkhammer (2005), Methane sources, distributions, and fluxes from cold vent sites at Hydrate Ridge, Cascadia Margin, *Global Biogeochem. Cycles*, *19*, GB2016, doi:10.1029/2004GB002266.

Heesemann, M., K. Juniper, M. Hoeberechts, M. Matabos, S. Mihaly, M. Scherwath, and R. Dewey (2013), Ocean networks Canada: Live sensing of a dynamic ocean system, Abstract EGU2013-6625 presented at EGU General Assembly Conference Abstracts, vol. 15, 6625 pp., EGU, Vienna, Austria, 7–12 Apr.

Henry, P., et al. (1996), Fluid flow in and around a mud volcano field seaward of the Barbados accretionary wedge: Results from Manon cruise, *J. Geophys. Res.*, *101*(B9), 20,297–20,323.

Holbrook, W. S., G. Kent, K. Keranen, H. P. Johnson, A. Trehu, H. Tobin, and J. Beeson (2012), Cascadia fore arc seismic survey: Open-access data available, *Eos Trans. AGU*, *93*(50), 521–522.

Homola, K., H. P. Johnson, and C. Hearn (2015), In situ measurements of thermal diffusivity in sediments of the methane-rich zone of Cascadia Margin, NE Pacific Ocean, *Elementa*, *3*(1), 000039.

Hornbach, M. J., N. L. Bangs, and C. Berndt (2012), Detecting hydrate and fluid flow from bottom simulating reflector depth anomalies, *Geology*, *40*(3), 227–230.

Hyndman, R. D. (2013), Downdip landward limit of Cascadia great earthquake rupture, *J. Geophys. Res. Solid Earth*, *118*, 5530–5549, doi: 10.1002/jgrb.50390.

Hyndman, R. D., et al. (1993), Tectonic sediment thickening, fluid expulsion, and the thermal regime of subduction zone accretionary prisms: The Cascadia margin off Vancouver Island, *J. Geophys. Res.*, *98*(B12), 21,865–21,876.

Johnson, H. P., E. A. Solomon, R. N. Harris, M. S. Salmi, and R. D. Berg (2013), Heat flow and fluid flux in Cascadia's seismogenic zone, *Eos Trans. AGU*, *94*(48), 457–458.

Johnson, J. E., C. Goldfinger, and E. Suess (2003), Geophysical constraints on the surface distribution of authigenic carbonates across the Hydrate Ridge region, Cascadia margin, *Mar. Geol.*, *202*(1), 79–120.
Joseph, C., K. A. Campbell, M. E. Torres, R. A. Martin, J. W. Pohlman, M. Riedel, and K. Rose (2013), Methane-derived authigenic carbonates from modern and paleoseeps on the Cascadia margin: Mechanisms of formation and diagenetic signals, *Palaeogeogr. Palaeoclimatol. Palaeoecol.*, *390*, 52–67.
Kannberg, P. K., A. M. Tréhu, S. D. Pierce, C. K. Paull, and D. W. Caress (2013), Temporal variation of methane flares in the ocean above Hydrate Ridge, Oregon, *Earth Planet. Sci. Lett.*, *368*, 33–42.
Lapham, L., R. Wilson, M. Riedel, C. K. Paull, and M. E. Holmes (2013), Temporal variability of in situ methane concentrations in gas hydrate-bearing sediments near Bullseye Vent, Northern Cascadia Margin, *Geochem. Geophys. Geosyst.*, *14*, 2445–2459, doi:10.1002/ggge.20167.
Leifer, I., and R. K. Patro (2002), The bubble mechanism for methane transport from the shallow sea bed to the surface: A review and sensitivity study, *Cont. Shelf Res.*, *22*(16), 2409–2428.
Leifer, I., and D. Culling (2010), Formation of seep bubble plumes in the Coal Oil Point seep field, *Geo Mar. Lett.*, *30*, 339–353.
Leifer, I., B. P. Luyendyk, J. Boles, and J. F. Clark (2006), Natural marine seepage blowout: Contribution to atmospheric methane, *Global Biogeochem. Cycles*, *20*, GB3008, doi:10.1029/2005GB002668.
Li, H. L., T. He, and G. D. Spence (2014), North Cascadia heat flux and fluid flow from gas hydrates: Modeling 3-D topographic effects, *J. Geophys. Res. Solid Earth*, *119*, 99–115, doi:10.1002/2013JB010101.
Liu, X., and P. B. Flemings (2006), Passing gas through the hydrate stability zone at southern Hydrate Ridge, offshore Oregon, *Earth Planet. Sci. Lett.*, *241*(1), 211–226.
MacKay, M. E., G. F. Moore, G. R. Cochrane, J. C. Moore, and L. D. Kulm (1992), Landward vergence and oblique structural trends in the Oregon margin accretionary prism: Implications and effect on fluid flow, *Earth Planet. Sci. Lett.*, *109*(3), 477–491.
Malinverno, A., M. Kastner, M. E. Torres, and U. G. Wortmann (2008), Gas hydrate occurrence from pore water chlorinity and downhole logs in a transect across the northern Cascadia margin (Integrated Ocean Drilling Program Expedition 311), *J. Geophys. Res.*, *113*, B08103, doi:10.1029/2008JB005702.
Mandal, R., P. Dewangan, T. Ramprasad, B. J. P. Kumar, and K. Vishwanath (2014), Effect of thermal non-equilibrium, seafloor topography and fluid advection on BSR-derived geothermal gradient, *Mar. Pet. Geol.*, *58A*, 368–381.
Martin, R. A., E. A. Nesbitt, and K. A. Campbell (2007), Carbon stable isotopic composition of benthic foraminifera from Pliocene cold methane seeps, Cascadia accretionary margin, *Palaeogeogr. Palaeoclimatol. Palaeoecol.*, *246*(2), 260–277.
McNeill, L. C., K. A. Piper, C. Goldfinger, L. D. Kulm, and R. S. Yeats (1997), Listric normal faulting on the Cascadia continental margin, *J. Geophys. Res.*, *102*(B6), 12,123–12,138
Moore, J. C., and P. Vrolijk (1992), Fluids in accretionary prisms, *Rev. Geophy.*, *30*(2), 113–135.
Moore, J. C., K. M. Brown, F. Horath, G. Cochrane, M. MacKay, and G. Moore (1991), Plumbing accretionary prisms: Effects of permeability variations, *Philos. Trans. R. Soc. London A*, *335*(1638), 275–288.
Nesbitt, E. A., R. A. Martin, and K. A. Campbell (2013), New records of Oligocene diffuse hydrocarbon seeps, northern Cascadia margin, *Palaeogeogr. Palaeoclimatol. Palaeoecol.*, *390*, 116–129.
Orange, D. L., B. G. McAdoo, J. C. Moore, H. Tobin, E. Screaton, H. Chezar, H. Lee, M. Reid, and R. Vail (1997), Headless submarine canyons and fluid flow on the toe of the Cascadia accretionary complex, *Basin Res.*, *9*(4), 303–312.
Phrampus, B. J., and M. J. Hornbach (2012), Recent changes to the Gulf Stream causing widespread gas hydrate destabilization, *Nature*, *490*(7421), 527–530.
Phrampus, B. J., M. J. Hornbach, C. D. Ruppel, and P. E. Hart (2014), Widespread gas hydrate instability on the upper US Beaufort margin, *J. Geophys. Res. Solid Earth*, *119*, 8594–8609, doi:10.1002/2014JB011290.
Riedel, M. (2007), 4D seismic time-lapse monitoring of an active cold vent, northern Cascadia margin, *Mar. Geophys. Res.*, *28*(4), 355–371.
Riedel, M., G. D. Spence, N. R. Chapman, and R. D. Hyndman (2001), Deep-sea gas hydrates on the northern Cascadia margin, *Leading Edge*, *20*(1), 87–109.
Riedel, M., I. Novosel, G. D. Spence, R. D. Hyndman, R. N. Chapman, R. C. Solem, and T. Lewis (2006), Geophysical and geochemical signatures associated with gas hydrate-related venting in the northern Cascadia margin, *Geol. Soc. Am. Bull.*, *118*(1–2), 23–38.
Riedel, M., A. M. Tréhu, and G. D. Spence (2010), Characterizing the thermal regime of cold vents at the northern Cascadia margin from bottom-simulating reflector distributions, heat-probe measurements and borehole temperature data, *Mar. Geophys. Res.*, *31*(1–2), 1–16.
Ritger, S., B. Carson, and E. Suess (1987), Methane-derived authigenic carbonates formed by subduction-induced pore-water expulsion along the Oregon/Washington margin, *Geol. Soc. Am. Bull.*, *98*, 147–156, doi:10.1130/0016-7606(1987)98<147MACFBS>2.0.CO;2.
Römer, M., H. Sahling, T. Pape, G. Bohrmann, and V. Spiess (2012a), Quantification of gas bubble emissions from submarine hydrocarbon seeps at the Makran continental margin (offshore Pakistan), *J. Geophys. Res.*, *117*, C10015, doi:10.1029/2011JC007424.
Römer, M., H. Sahling, T. Pape, A. Bahr, T. Feseker, P. Wintersteller, and G. Bohrmann (2012b), Geological control and magnitude of methane ebullition from a high-flux seep area in the Black Sea: The Kerch seep area, *Mar. Geol.*, *319*, 57–74.
Ryan, W. B. F., et al. (2009), Global multi-resolution topography synthesis, *Geochem. Geophys. Geosyst.*, *10*, Q03014, doi:10.1029/2008GC002332.
Saffer, D. M. (2014), The permeability of active subduction plate boundary faults, *Geofluids*, *15*, 193–215.
Salmi, M. S., H. P. Johnson, I. Leifer, and J. E. Keister (2011), Behavior of methane seep bubbles over a pockmark on the Cascadia continental margin, *Geosphere*, *7*(6), 1273–1283.
Satake, K., and B. F. Atwater (2007), Long-term perspectives on giant earthquakes and tsunamis at subduction zones, *Annu. Rev. Earth Planet. Sci.*, *35*, 349–374.
Sauter, E. J., S. I. Muyakshin, J.-L. Charlou, M. Schlüter, A. Boetius, K. Jerosch, E. Damm, J.-P. Foucher, and M. Klages (2006), Methane discharge from a deep-sea submarine mud volcano into the upper water column by gas hydrate-coated methane bubbles, *Earth Planet. Sci. Lett.*, *243*(3), 354–365.
Schneider von Deimling, J., and C. Papenberg (2012), Detection of gas bubble leakage via correlation of water column multibeam images, *Ocean Sci.*, *8*(2), 175–181.
Schneider von Deimling, J., J. Greinert, N. R. Chapman, W. Rabbel, and P. Linke (2010), Acoustic imaging of natural gas seepage in the North Sea: Sensing bubbles controlled by variable currents, *Limnol. Oceanogr. Methods*, *8*(5), 155–171.
Schneider von Deimling, J., G. Rehder, J. Greinert, D. F. McGinnnis, A. Boetius, and P. Linke (2011), Quantification of seep-related methane gas emissions at Tommeliten, North Sea, *Cont. Shelf Res.*, *31*(7–8), 867–878.
Shi, Y., and C. Y. Wang (1994), Model studies of advective heat flow associated with compaction and dehydration in accretionary prisms, *J. Geophys. Res.*, *99*(B5), 9319–9325.

Skarke, A., C. Ruppel, M. Kodis, D. Brothers, and E. Lobecker (2014), Widespread methane leakage from the sea floor on the northern US Atlantic margin, *Nat. Geosci.*, *7*, 657–661.

Sluijs, A., et al. (2006), Subtropical Arctic Ocean temperatures during the Palaeocene/Eocene thermal maximum, *Nature*, *441*(7093), 610–613.

Solomon, E. A., M. Kastner, H. Jannasch, Y. Weinstein, and G. Robertson (2008), Dynamic fluid flow and chemical fluxes associated with a seafloor gas hydrate deposit on the northern Gulf of Mexico slope, *Earth Planet. Sci. Lett.*, *270*(1–2), 95–105.

Suess, E., et al. (1999), Gas hydrate destabilization: Enhanced dewatering, benthic material turnover and large methane plumes at the Cascadia convergent margin, *Earth Planet. Sci. Lett.*, *170*, 1–15.

Suess, E., et al. (2001), Sea floor methane hydrates at hydrate ridge, Cascadia margin, in *Natural Gas Hydrates: Occurrence, Distribution, and Detection*, edited by C. K. Paull and W. P. Dillon, pp. 87–98, AGU, Washington, D. C., doi:10.1029/GM124p0087.

Teichert, B. M. A., A. Eisenhauer, G. Bohrmann, A. Haase-Schramm, B. Bock, and P. Linke (2003), U/Th systematics and ages of authigenic carbonates from Hydrate Ridge, Cascadia convergent margin: Recorders of fluid composition and sea-level changes, *Geochim. Cosmochim. Acta*, *67*, 3845–3857.

Thomsen, L., C. Barnes, M. Best, R. Chapman, B. Pirenne, R. Thomson, and J. Vogt (2012), Ocean circulation promotes methane release from gas hydrate outcrops at the NEPTUNE Canada Barkley Canyon node, *Geophys. Res. Lett.*, *39*, L16605, doi:10.1029/2012GL052462.

Torres, M. E., K. Wallmann, A. M. Tréhu, G. Bohrmann, W. S. Borowski, and H. Tomaru (2004), Gas hydrate growth, methane transport, and chloride enrichment at the southern summit of Hydrate Ridge, Cascadia margin off Oregon, *Earth Planet. Sci. Lett.*, *226*(1), 225–241.

Torres, M. E., R. W. Embley, S. G. Merle, A. M. Trehu, R. W. Collier, E. Suess, and K. U. Heeschen (2009), Methane sources feeding cold seeps on the shelf and upper continental slope off central Oregon, USA, *Geochem. Geophys. Geosyst.*, *10*, Q11003, doi:10.1029/2009GC002518.

Trehu, A. M., et al. (2004). Three-dimensional distribution of gas hydrate beneath southern Hydrate Ridge: Constraints from ODP Leg 204, *Earth Planet. Sci. Lett.*, *222*(3), 845–862.

Trehu, A. M., M. E. Torres, G. Bohrmann, and F. Colwell (2006), Leg 204 synthesis: Gas hydrate distribution and dynamics in the central Cascadia accretionary complex, in *Proceedings of Ocean Drilling Program*, *Sci. Results*, vol. 204, edited by A. M. Tréhu, et al., pp. 1–40, Ocean Drill. Program, College Station, Tex., doi:10.2973/odp.proc.sr.204.101.2006.

Tryon, M. D., K. M. Brown, and M. E. Torres (2002), Fluid and chemical flux in and out of sediments hosting methane hydrate deposits on Hydrate Ridge, OR. II: Hydrological processes, *Earth Planet. Sci. Lett.*, *201*, 541–557, doi:10.1016/S0012-821X (02)00732-X.

Wang, K. (1994), Kinematic models of dewatering accretionary prisms, *J. Geophys. Res.*, *99*(B3), 4429–4438.

Wang, K., R. D. Hyndman, and E. E. Davis (1993), Thermal effects of sediment thickening and fluid expulsion in accretionary prisms: Model and parameter analysis, *J. Geophys. Res.*, *98*(B6), 9975–9984.

Wright, J. D., and M. F. Schaller (2013), Evidence for a rapid release of carbon at the Paleocene-Eocene thermal maximum, *Proc. Natl. Acad. Sci., U. S. A.*, *110*(40), 15,908–15,913.

Zachos, J. C., et al. (2005), Rapid acidification of the ocean during the Paleocene-Eocene thermal maximum, *Science*, *308*(5728), 1611–1615.